



Share Your Innovations through JACS Directory

Journal of Nanoscience and Technology

Visit Journal at <http://www.jacsdirectory.com/jnst>

Morphology Manipulation and Related Properties of High Crystalline Bi₂S₃ Nanorods by Reflux Approach

J. Arumugam, A. Dhayal Raj*, A. Albert Irudayaraj

PG & Research Department of Physics, Sacred Heart College (Autonomous), Tirupattur – 635 602, Tamilnadu, India.

ARTICLE DETAILS

Article history:

Received 11 September 2018

Accepted 13 October 2018

Available online 08 November 2018

Keywords:

Bi₂S₃ Nanorods

XRD

HRTEM

Reflux Approach

ABSTRACT

One dimensional Bi₂S₃ nanorods have been successfully synthesized by a very simple reflux method with different precursor concentration for 2 hours at 180 °C. The as-synthesized Bi₂S₃ powders were characterized by X-ray diffraction (XRD), high resolution scanning electron microscope (HRSEM), high resolution transmission microscope (HRTEM), UV-Vis spectrometer, Fourier transform infrared (FTIR) spectrometer. X-ray diffraction (XRD) results show that the resulting nanocrystals have an orthorhombic structure. X-ray diffraction patterns indicate a polycrystalline nature and the crystallite sizes seem increase with increase in the concentration. The HRSEM and HRTEM images reveal that the diameter of the nanorods increase with increasing concentration of the precursor. Morphological analysis reveals that the as-prepared Bi₂S₃ nanorods can be tuned to morphology by varying precursor concentration from 0.01 M to 0.001 M. The bismuth nitrate, which is known to be a linear polymer, plays a critical role as a precursor and a template for the growth of uniform Bi₂S₃ nanorods. Bi₂S₃ nanorods are good absorbents of solar radiation and hence can be used in solar cells.

1. Introduction

Environmental problems associated with organic pollutants and toxic water pollutants provide the impetus for sustained fundamental and applied research in the area of environmental remediation. Recently, great expectations concerning the application of nanomaterials as promising materials for environmental safety have been rising. Various morphologies of nanostructures have been synthesized via diverse methods, which are expected to offer new opportunities for applications in the emerging fields of nanoscience and nanotechnology. The fine control of the fabrication of semiconductor nanocrystals [1], metal nanocrystals [2], and other inorganic nanomaterials [3] has attracted significant attention, which may add alternative variables in tailoring the properties of nanomaterials and provide more possibilities in fabrication of nanodevices. Due to the strong correlation between the properties of a materials and the shape, size, and structure of materials, designing and preparing novel nano and micro structured materials has been intensively pursued not only for fundamental scientific interest but also for their applications in various fields. Semiconductor nanocrystals have attracted great attention on their synthesis and characterization because of the unique size- and shape-dependent properties and could be widely used in photocatalyst, solar cell, lasers, biomedical probes, light emitting diodes, photoluminescence and optoelectronic devices, etc. [4]. Bismuth sulfide (Bi₂S₃) is a semiconductor of great interest because of its unique optical and electronic properties [5]. Bismuth sulfide (Bi₂S₃) nanoparticles can be used in various fields such as thermoelectric devices [6], photovoltaics [7], nonlinear absorption [8], biomolecule detection [9], photodiode array and infrared spectroscopy [10, 11]. Till date various morphologies of Bi₂S₃ such as nanorods [12], nanoparticles [13], nanowires and nanoflowers [14], have been synthesized by using a variety of methods such as hydrothermal route [15], precipitation [16], and microwave irradiation [17]. Development of simple, effective and template-free methods for fabricating Bi₂S₃ nanostructure is of great importance to nanotechnology and remains a key research challenge.

It is generally accepted that low temperature synthesis in aqueous solutions is highly desirable because it represents an environmentally friendly approach of practical significance. Recently, Rong Chen et al., [18] have reported the large scale synthesis of bismuth sulfide nanorods by a

microwave approach; using different reaction parameters like reaction time, surfactants, and solvents. Pengfei Hu et al., [19] have prepared Bi₂S₃ nanorods by a simple solvothermal route and their electrochemical hydrogen storage performance has been reported. A.J. Pal et al., [20] have reported the use of metal-semiconductor schottky junctions in a conjugated polymer matrix as solar cells. They have formed the Schottky junctions through an intimate contact between Bi₂S₃ nanorods and gold nanoparticles, following a one-pot synthesis route. Pallavi N.Sakariya et al., [21] have reported the preparation of Bi₂S₃ nanorods at room temperature. Zhendong Liu et al., [22] have synthesized Bi₂S₃ nanorods and nanoflowers by reflux process for flexible near infrared laser detectors and visible light photodetectors. They have reported that Bi₂S₃ nanorods based on visible light photodetector exhibits higher LDR value than other Bi₂S₃ based photodetectors. Bin Xue et al., [23] have prepared bismuth sulfide (Bi₂S₃) nanorods by gelatin assisted green solution process under microwave irradiation. They have reported that gelatin plays an important role for the formation of the Bi₂S₃ nanorods for changing the concentration in photoelectric nanodevices.

In this work, Bi₂S₃ nanorods have been prepared with different precursor concentration by reflux method. The products were characterized by for their fundamental properties and the effect of precursor concentration has been investigated. The results showed that the precursor concentration would affect the morphology of the resulting products remarkably.

2. Experimental Methods

All the reagents were of analytical grade and were used directly without further purification. In a typical experiment, 0.001 M of bismuth nitrate and citric acid were mixed with 0.003 M thiourea and 0.007 M cetyltrimethylammounium bromide in 100 mL of DMF. The mixture was stirred and sonicated until all the chemicals were dissolved. The mixture was refluxed at 180 °C for 2 hours with continuous stirring and after cooling down naturally to the room temperature, the mixture was centrifuged and the black color solid product was collected. The solid product was then washed several times in acetone and water. Finally, the solid product was dried in a hot air oven. In order to analyze the effect of precursor concentration, the same procedure was followed by increasing the bismuth nitrate concentration alone to 0.01 M. The synthesized samples were further characterized by power X-ray diffraction, HRSEM, EDAX, HRTEM, SAED, UV-Vis spectroscopy and Fourier-transform infrared spectroscopy.

*Corresponding Author: dhayalraj03@gmail.com (A. Dhayal Raj)

3. Results and Discussion

3.1 Structural Analysis

Uniform bismuth sulfide nanorods were obtained by simple reflux method as confirmed by the powder XRD pattern shown in Fig. 1. The polycrystalline nature of the samples have been confirmed through the appearance of multiple peaks [24]. All the diffraction peaks can be readily indexed to the orthorhombic phase of the bismuth sulfide. The lattice constants a , b and c with values 11.14 Å, 11.30 Å and 3.98 Å respectively, are in the good agreement with the standard data (JCPDS card No. 170320). In Fig. 1, the intensity of (0 4 0) peak is most intense as compared with the other peaks. This indicates that the orientation of the grain growth is preferably along (0 4 0) direction. The crystallite size of the Bi_2S_3 nanorods is determined from the XRD spectra by using Scherrer's formula, $D = K\lambda/\beta\cos\theta$, where, D is the average crystalline size, k is a constant whose value is typically 0.9 for non-spherical crystals, β is the full width at half maximum (FWHM) of the diffraction peak (in radians) that has the maximum intensity in the diffraction pattern, λ is the wavelength of incident X-ray beam (0.154184 nm), and θ is diffraction angle or Bragg angle. It is well known that the diffraction peak width is inversely proportional to the crystallite size. The grain size calculated for the samples prepared with 0.01 M and 0.001 M were found to be 36 nm and 33 nm respectively. No impurities can be detected in these patterns which indicate that pure Bi_2S_3 can be obtained under the current synthesis conditions.

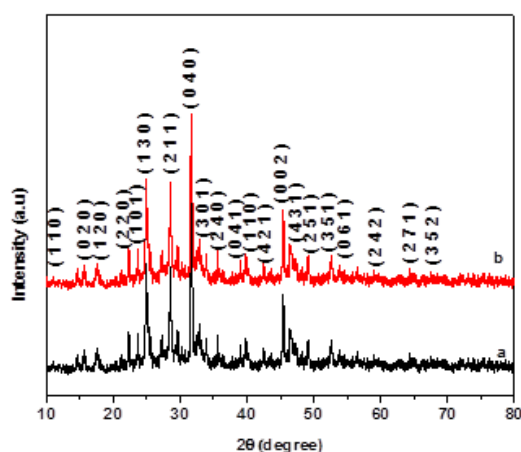


Fig. 1 XRD Pattern of as-prepared Bi_2S_3 nanorods prepared with different precursor concentrations (a) 0.01 M and (b) 0.001 M

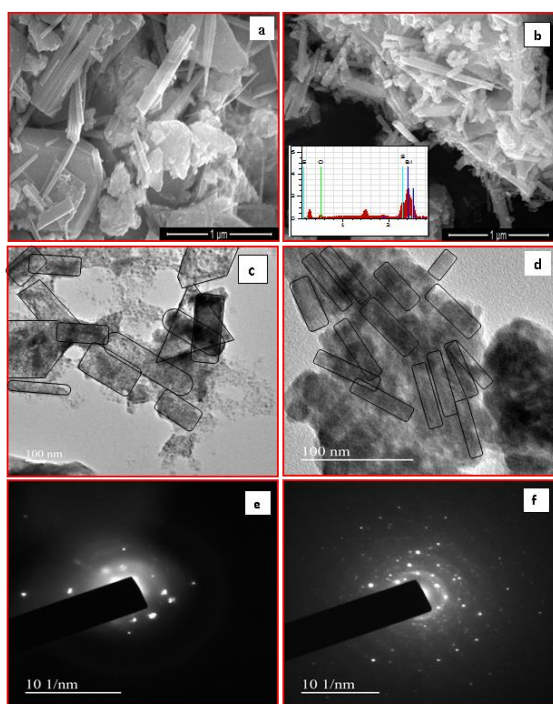


Fig. 2 HR-SEM and HR-TEM image of the Bi_2S_3 nanorods prepared with different precursor concentrations (a), (c) 0.01 M, and (b), (d) 0.001 M by reflux method, (e) and (f) the SAED patterns of the as-prepared Bi_2S_3 nanorods prepared with different concentration of 0.01 M and 0.001 M
<https://doi.org/10.30799/jnst.159.18040516>

3.2 Morphological Analysis

The effects of precursor concentration on the morphology of the prepared Bi_2S_3 samples were investigated through HRSEM and HRTEM analysis. The HRSEM micrographs of both the samples shows nanorod like formations (Fig. 2 (a and b)). However, the samples prepared with higher concentration of 0.01 M shows plate like formation along with nanorods as shown in Fig. 2a. The EDAX pattern presented as insert image in Fig. 2b confirms the formation of Bi_2S_3 . It also reveals the purity of the sample. The dimension of the nanorods as calculated from the HRTEM in Fig. 2(c and d) were found to be 312 nm length and 131 nm breadth for sample prepared with 0.01 M whereas 69 nm length and 23 nm breadth for samples prepared with 0.001 M concentration. Images in Fig. 2(e and f) correspond to the SAED pattern of the samples. These images clearly reveal the good crystalline nature of the sample.

3.3 Optical Analysis

The optical properties of Bi_2S_3 nanorods were investigated using UV-Vis spectra. The optical bandgap (E_g) of the semiconductor material could be calculated from the equation of $\alpha h\nu = A(h\nu - E_g)^n$, where, α , ν , E_g and A were the absorption coefficient, light frequency, band gap energy and a constant, respectively. Moreover, n depends on the nature of transitions and may takes values as 1/2 and 2 for allowed direct and indirect transitions respectively. It is possible to determine the nature of the transitions involved by plotting the graphs of $(\alpha h\nu)^n$ versus $(h\nu)$ for the different values of n as described above. The bandgap may be estimated from the intercept of the extrapolating linear fit to the experimental data of the Tauc plot. Band gap estimated for the samples prepared with 0.01 M and 0.001 M concentrations were 1.84 eV and 1.85 eV respectively (Fig. 3). The estimated bandgap were found to be very close to reported for Bi_2S_3 nanostructures [25, 26]. The higher values of the bandgap energy when compared with the corresponding bulk value can be attributed to the nanocrystalline nature of the sample.

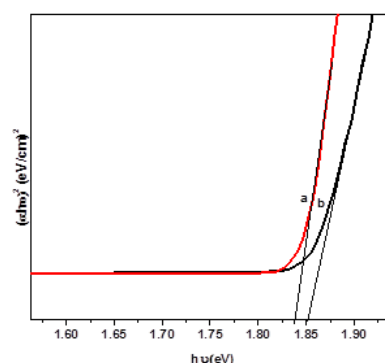


Fig. 3 The plot of $(\alpha h\nu)^2$ versus $(h\nu)$ of Bi_2S_3 nanorods prepared with different precursor concentrations (a) 0.01 M and (b) 0.001 M

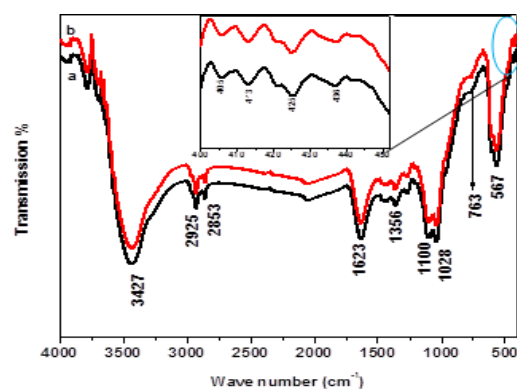


Fig. 4 FTIR spectra of Bi_2S_3 nanorods prepared with different precursor concentrations (a) 0.01 M and (b) 0.001 M

3.4 Functional Analysis

The composition and quality of the sample were analyzed by the FTIR spectroscopy. Fig. 4 (a and b) shows the FTIR spectra of the samples obtained for different precursor concentrations 0.01 M and 0.001 M respectively. The broad band at 3000–3600 cm^{-1} is the result of stretching of H_2O , while the band at 1623 cm^{-1} correspond to the bending vibration of H_2O [27]. Moreover, the peaks at 2925 cm^{-1} and 2853 cm^{-1} could be attributed to the characteristic asymmetric and symmetric stretching in C-H and N-H vibration of amino group [28]. The peaks at 1028 cm^{-1} and 763 cm^{-1} are for C-H in-plane deformation and out-of plane stretching,

respectively [29]. The weak peak around 1356 cm^{-1} appearing in all the samples may be assigned to C-S and C-N stretching vibration [30]. A strong intensity band present in the region 567 cm^{-1} may be attributed to the symmetric and asymmetric vibrations of sulphur, while a medium intensity band in the region $460\text{--}403\text{ cm}^{-1}$ can be assigned to bismuth [31].

4. Conclusion

High-quality Bi_2S_3 nanorods have been successfully prepared by a simple reflux approach with different precursor concentration. Reflux method is a convenient, mild, efficient and environmental friendly route for producing nanocrystalline metal sulfides. From the investigation on the effects of precursor concentration, it was concluded that the increase in the precursor concentration resulted in higher degree of crystallinity. The XRD pattern revealed that the prepared Bi_2S_3 nanocrystals are of orthorhombic phase and their sizes were in the range of 32 nm to 36 nm and the prepared samples exhibited a polycrystalline nature. The Bi_2S_3 nanorods prepared with a lower precursor concentration showed smaller sized rods having 23 nm diameter and 69 nm length. These nanorods also had narrow diameter distribution and high growth density. The vibrational behaviors of the bonds are further analyzed using FTIR and the strong peaks around 460 cm^{-1} and 567 cm^{-1} confirmed the formation of Bi_2S_3 . Thus, this work sheds light on the factors that govern the growth of well-aligned Bi_2S_3 nanorod and gains access to the controlled fabrication of 1D alignment of other materials on its applications.

Acknowledgements

The authors would like to acknowledge the management, Sacred Heart College for extending support to complete this work successfully.

References

- [1] X.G. Peng, L. Manna, W.D. Yang, J. Wickham, E. Scher, et al., Shape control of CdSe nanocrystals, *Nature* 404 (2000) 59–61.
- [2] T.S. Ahmadi, Z.L. Wang, T.C. Green, A. Henglein, M.A. Sayed, Shape-controlled synthesis of colloidal platinum nanoparticles, *Science* 272 (1996) 1924–1926.
- [3] M. Li, H. Schnablegger, S. Mann, Coupled synthesis and self-assembly of nanoparticles to give structures with controlled organization, *Nature* 402 (1999) 393–395.
- [4] C.L. Feng, X. Zhong, M. Steinhart, A.M. Caminade, J.P. Majoral, W. Knoll, Graded-bandgap quantum-dot-modified nanotubes: A sensitive biosensor for enhanced detection of DNA hybridization, *Adv. Mater.* 19 (2007) 1933–1936.
- [5] D. Arivuoli, F.D. Gnanam, P. Ramasamy, Growth and microhardness studies of chalcogenides of arsenic, antimony and bismuth, *J. Mater. Sci. Lett.* 7 (1998) 711–713.
- [6] M. Yousefi, M. Salavati-Niasari, F. Gholamian, D. Ghanbari, A. Aminifazl, Polymeric nanocomposite materials: Synthesis and thermal degradation of acrylonitrile–butadiene–styrene/tin sulfide (ABS/SnS), *Inorg. Chim. Acta.* 371 (2011) 1–5.
- [7] H. Cheng, B. Huang, X. Qin, X. Zhang, Y. Dai, A controlled anion exchange strategy to synthesize Bi_2S_3 nanocrystals/ BiOCl hybrid architectures with efficient visible light photoactivity, *Chem. Commun.* 48 (2012) 97–99.
- [8] X.Y. Yang, W.D. Xiang, H.J. Zhao, H.T. Liu, X.Y. Zhang, X.J. Liang, Nonlinear saturable absorption of the sodium borosilicate glass containing Bi_2S_3 nanocrystals using Z-scan technique, *J. Alloys Compd.* 509 (2011) 7283–7289.
- [9] L. Cademartiri, F. Scotognella, P.G. O'Brien, B.V. Lotsch, J. Thomson, S. Petrov, N.P. Kherani, G.A. Ozin, Cross-Linking Bi_2S_3 Ultrathin Nanowires: A Platform for Nanostructure Formation and Biomolecule Detection, *Nano Lett.* 9 (2009) 1482–1486.
- [10] S.H. Pawar, P.N. Bhosale, M.D. Uplane, S. Tanhankar, Growth of Bi_2S_3 film using a solution-gas interface techniques, *Thin Solid Films* 110 (1983) 165–170.
- [11] J. Grigas, E. Talik, V. Lazauskas, X-ray photoelectron spectra and electronic structural of Bi_2S_3 crystals, *Phys. Status Solid B.* 232 (2002) 220–230.
- [12] Z. Liu, J. Fang, W. Xu, X. Xu, S. Wu, X. Zhu, Low temperature hydrothermal synthesis of Bi_2S_3 nanorods using nanosheets as self-sacrificing templates BiOI , *Mater. Lett.* 88 (2012) 82–85.
- [13] L. Shi, D. Gu, W. Li, L. Han, H. Wei, B. Tu, R. Che, Synthesis of monodispersed ultrafine Bi_2S_3 nanocrystals, *J. Alloys Compd.* 509 (2011) 9382–9386.
- [14] C.J. Tang, G.Z. Wang, H.Q. Wang, Y.X. Zhang, G.H. Li, Facile synthesis of Bi_2S_3 nanowire arrays, *Mater. Lett.* 62 (2008) 3663–3665.
- [15] A. Phuruangrat, T. Thongtem, S. Thongtem, Characterization of Bi_2S_3 nanorods and nano-structured flowers prepared by a hydrothermal method, *Mater. Lett.* 63 (2009) 1496–1498.
- [16] Y. Jiang, Y.J. Zhu, Z.L. Xu, Rapid synthesis of Bi_2S_3 nanocrystals with different morphologies by microwave heating, *Mater. Lett.* 60 (2006) 2294–2298.
- [17] T. Thongtem, A. Phuruangrat, S. Wannapop, S. Thongtem, Characterization of Bi_2S_3 with different morphologies synthesized using microwave radiation, *Mater. Lett.* 64 (2010) 122–124.
- [18] J. Wu, F. Qin, G. Chen, H. Li, J. Zhang, Y. Xie, et al., Large-scale synthesis of bismuth sulfide nanorods by microwave irradiation, *J. Alloys Compd.* 509 (2011) 2116–2126.
- [19] P. Hu, Y. Cao, B. Lu, Flower like assemblies of Bi_2S_3 nanorods by Solvothermal route and their electrochemical hydrogen storage performance, *Mater. Lett.* 106 (2013) 297–300.
- [20] S.K. Saha, A.J. Pal, Schottky diodes between Bi_2S_3 nanorods and metal nanoparticles in a polymer matrix as hybrid bulk-heterojunction solar cells, *J. Appl. Phys.* 118 (2015) 014503–014513.
- [21] M.P. Deshpande, P.N. Sakariya, S.V. Bhatt, N. Garg, K. Patel, S.H. Chai, Characterization of Bi_2S_3 nanorods prepared at room temperature, *Mater. Sci., Semi. Proc.* 21 (2014) 180–185.
- [22] J. Chao, S. Xing, Z. Liu, X. Zhang, Y. Zhao, L. Zhao, Q. Fan, Large-scale synthesis of Bi_2S_3 nanorods and nanoflowers for flexible near infrared laser detectors and visible light photodetectors, *Mater. Res. Bull.* 98 (2018) 194–199.
- [23] B. Xue, T. Sun, F. Mao, J. Xie, Gelatin-assisted green synthesis of bismuth sulfide nanorods under microwave irradiation, *Mater. Lett.* 122 (2014) 106–109.
- [24] G. Nagaraj, A. Dhayal Raj, A. Albert Irudayaraj, Next generation of pure titania nanoparticles for enhanced solar-light photocatalytic activity, *J. Mater. Sci. Mater. Electron.* 29 (2018) 4373–4381.
- [25] C. Ye, G. Meng, Z. Jiang, Y. Wang, G. Wang, L. Zhang, Rational Growth of Bi_2S_3 nanotubes from Quasi-two-dimensional Precursors, *J. Am. Chem. Soc.* 124 (2002) 15180–15181.
- [26] J. Arumugam, A. Dhayal Raj, A. Albert Irudayaraj, M. Thambidurai, Solvothermal synthesis of Bi_2S_3 nanoparticles and nanorods towards solar cell application, *Mater. Lett.* 220 (2018) 28–31.
- [27] G. Biasotto, A.Z. Simoes, C.R. Foschini, S.G. Antonio, M.A. Zaghet, J.A. Verela, A novel synthesis of perovskite bismuth ferrite nanoparticles, *J. Process. App. Ceramics.* 5 (2011) 171–179.
- [28] T. Thongtem, C. Pilapong, J. Kavinchien, A. Phuruangrat, S. Thongtem, Microwave-assisted hydrothermal synthesis of Bi_2S_3 nanorods in flower-shaped bundles, *J. Alloys Compd.* 500 (2010) 195–199.
- [29] J. Ota, S.K. Srivastav, Polypyrrole Coating of tartaric acid-assisted synthesized Bi_2S_3 nanorods, *J. Phys. Chem. C* 111 (2007) 12260–12264.
- [30] C. Tang, C. Wang, F. Su, C. Zang, Y. Yang, Z. Zong, Y. Zhang, Controlled synthesis of urchin-like Bi_2S_3 via hydrothermal method, *Solid State Sci.* 12 (2010) 1352–1356.
- [31] A.K. Jain, R. Bohra, Synthesis and characterization of some methylbismuth(III) O,O-alkylenedithiophosphates: convenient transformation of $[\text{MeBi}\{\text{S}_2\text{PO}(\text{CH}_2)_4\text{O}\}_2]$ and $[\text{MeBi}\{\text{S}_2\text{POCH}(\text{CH}_3)\text{CH}_2\text{C}(\text{O})(\text{CH}_3)_2\}_2]$ to pure Bi_2S_3 , *Appl. Organometal. Chem.* 20 (2006) 411–415.